disturbed high-cold meadow area, the original vegetation is very difficult to restore although its surface landscape can be restored to a certain degree. Borrow pits and piling grounds have great destruction to the high-cold meadow, the high-cold meadow ecosystem almost cannot be restored by natural processes, therefore, great efforts should be made to avoid setting up borrow ground in the high-cold meadow region.

Acknowledgements This work was supported by the National Natural Science Foundation of China (Grant Nos. 90102001 and 30270255) and the Key Projection of Knowledge Innovation Engineering, Chinese Academy of Sciences (Grant No. KZCX1-SW004).

References

1. Wu Qingbo, Zhu Yuanlin, Liu Yongzhi, Evaluating model of frozen soil environment change under engineering actions, Sciences in China, Series D, 2002, 45(10): 893—902.
2. Zhou Youwu, Cheng Guodong, Guo Dongxing et al., Research status and and tasks of permafrost, in Collected Papers of the 4th National Conference on Glaciology and Geocryology (Geocryology), Beijing: Science Press, 1990, 171—176.
3. Boughton, D. A., Smith, E. R., O'Neill, R. V., Regional vulnerability: a conceptual framework, Ecosystem Health, 1999, 5: 312—322.
4. Calow, P., Ecosystem health: a critical analysis of concept, in Evaluating and Monitoring the Health of Large-scale Ecosystems (eds. Rapport, D. J., Gaudet, C. L., Calow, P.), Heidelbug: Springer-Verlag, 1995, 33—42.
5. Wu Qingbo, Shi Bing, Liu Yongzhi, Interaction study of permafrost and highway along Qinghai-Xizang Highway, Sciences in China, Series D, 2002, 46(2): 97—105.
6. Zhao Lin, Chen Guichen, Cheng Guodong et al., Permafrost: status, variation and impacts, in Mountain Geoecology and Sustainable Development of the Tibetan Plateau (eds. Zheng Du, Zhang Qingsong, Shao Hong), Netherlands: Kluwer Academic Publishers, 2000, 113—137.
7. Wang Guoshang, Jin Huijun, Liu Qin et al., Permafrost changes and its environmental significance along the Qinghai-Tibet highway line, Journal of Glaciology and Geocryology, 1998, 20(4): 444—450.
8. Wang Shaoling, Zhao Xiufeng, Permafrost environmental changes in the island permafrost region at the south section of the Qinghai-Tibet Highway, Journal of Glaciology and Geocryology, 1997, 19(3): 231—239.
9. Li Wenhua, Zhou Xingmin, Ecosystem and Optimization Use Pattern on Qinghai-Tibet Plateau, Guangzhou: Guangdong Science and Technology Press, 1998, 19—67.
10. Zhou Xingmin, Kobresia Meadow in China, Beijing: Science Press, 2001, 188—206.
11. Chen Xiaouana, Gou Xinjing, Eco-Environment in the Nature Reserve of Three River Source, Xining: Qinghai People's Publishing House, 2002, 240.
12. Zhao Lin, Cheng Guodang, Li Shuxun et al., Thawing and freezing processes of active layer in Wudaoliang region of Tibetan Plateau, Chinese Science Bulletin, 2000, 45(23): 2181—2186.

(Received December 1, 2003; accepted March 11, 2004)

Chinese Science Bulletin 2004 Vol. 49 No. 16 1750—1757

Zircon SHRIMP dating of sodium alkaline rocks from Maomaogou area of Huili County in Panxi, SW China and its geological implications

LIU Hongying, XIA Bin & ZHANG Yuquan

Guangzhou Institute of Geochemistry, Chinese Academy of Sciences, Guangzhou 510640, China
Correspondence should be addressed to Liu Hongying (e-mail: Liuhy@gig.ac.cn)

Abstract **Alkali-feldspar syenites from the Maomaogou area of Huili County in Panxi of Sichuan Province, SW China are sodium alkaline rocks, the minerals of which are mainly composed of calcic ferroaugite, ferroamphibole and biotite. Most of the zircons (>80%) selected for SHRIMP U-Pb dating are magmatic compound zircons and they have relict inner cores and growing outer shells. The age of zircon SHRIMP U-Pb dating is 224±8 Ma, suggesting that the Maomaogou alkali-feldspar syenite was formed in the late Triassic period. At the same time, two old age periods of relict cores of zircon are determined, they are the Archean age (2692—2818 Ma) and Neoproterozoic age (622—691 Ma), respectively. These periods indicate that the cores derived from the crystal basement. Furthermore, the Archean age of zircon provides the first reliable SHRIMP U-Pb zircon dating evidence of >2.8 Ga basement in the Xikang-Yunnan Axis of southwest China.**

Keywords: SHRIMP dating, zircon, alkali-feldspar syenite, Maomaogou area, Sichuan Province.

DOI: 10.1360/03wd0656

Alkaline rocks are often associated with extensional tectonics and regarded as the characteristic products occurring in continental margins or rift zones[1]. They were usually generated in deep-large-fault zone and closely connected with basic/ultrabasic rocks in space. Therefore, alkaline rocks are of significance in tectonic petrology. At the beginning of the 1980s, geological and geophysical studies were performed in Panzhihua-Xichang paleo-rift zone (Panxi rift zone). However, these studies only involved geology and petrochemistry of the Maomaogou ring alkali complexes[2,3]. The geochronological study was conducted during the 1990s. The biotite K-Ar[4] and $^{40}Ar/^{39}Ar$ plateau ages[5] reported on the Maomaogou alkaline rocks are equal or older than the age of the late Permian Emeishan basalts. To obtain the crystallization time consistent with the geological observation, we determined the zircon SHRIMP U-Pb dating for the Maomaogou alkali-feldspar syenites.

1 Geological setting and sample description

The studied area is located at the middle part of the Panxi rift, which is controlled by Anning river-Yimen deep-fault zone. The Maomaogou plutons are situated in the east of Longzhou Mountains and show ring lens with NS orientation long axes. They are about 15 km in length and 23 km in width, and the outcropping area is about 35 km^2 (Fig. 1). The complexes intruded into the late Permian Emeishan basalt and lower Ordovician Hongshiya limestone and sandstone. Some basaltic xenoliths were found in the inner contact zone. Maomaogou alkaline complexes mainly consist of alkaline gabbros, alkali-feldspar syenites and nordmarkites. The zircons for SHRIMP U-Pb dating were separated from alkali-feldspar syenites. The alkali-feldspar syenite is gray or gray-black, shows middle-coarse granular, hypidiomorphic columner granular texture, and mainly consists of microcline, albite, nepheline, hedenbergite, ferropargasite and miner biotite. The microprobe analyses were carried out for the pyroxene and amphibole minerals. The results calculated by O = 6 and O = 23 suggest that they are hedenbergite and ferropargasite respectively (Table 1), which is consistent with the results in ref. [3].

Major-, and trace-elemental and Sm-Nd, Rb-Sr isotopic compositions are presented in Table 2. Distributions of the major-elements of these rocks are low SiO_2, high

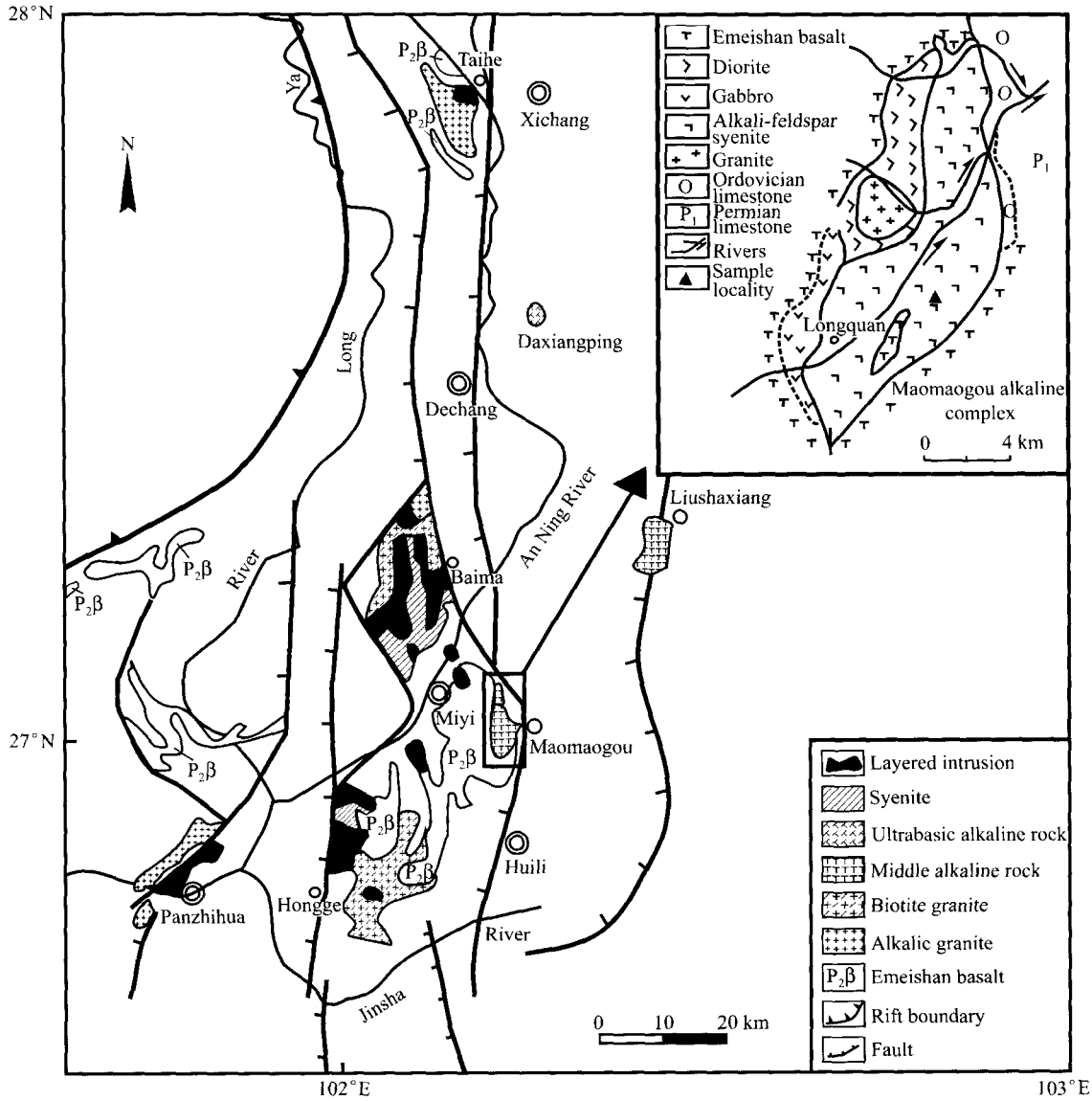

Fig. 1. Simplified geological map of Panxi area, Sichuan Province of SW China (modified from ref. [3]). The upper right inset is the geological map of the Maomaogou alkaline complexes. SGT, Songpan-Ganze Terrane; YB, Yangtze Block.

Table 1 Representative microprobe analyses of pyroxene and hornblende from Maomaogou alkaline feldspar syenite (%)

Lithology	Hedenbergite										Ferropargasite						
Sample	Sm-1	Sm-2	Sm-3	Sm-4	Sm-5	Sm-6	Sm-7	Sm-8	Sm-9	Sm-10	Sm-1	Sm-2	Sm-3	Sm-4	Sm-5	Sm-6	Sm-7
SiO_2	48.62	48.08	48.52	50.21	49.42	48.35	48.30	49.14	48.57	49.36	39.28	39.29	39.25	39.56	38.90	39.41	39.09
TiO_2	0.25	0.31	0.41	0.35	0.30	0.28	0.36	0.33	0.33	0.38	2.88	3.01	2.98	4.98	2.81	3.98	2.91
Al_2O_3	1.05	1.19	1.00	1.29	1.17	1.12	1.09	1.24	1.03	1.15	9.56	10.61	10.73	10.48	10.50	10.61	10.55
FeO[a)]	17.16	16.39	21.13	16.87	17.01	16.77	18.76	16.63	19.15	19.00	24.54	22.56	23.81	23.79	24.56	23.80	23.56
MnO	1.04	1.10	1.35	0.96	1.00	1.07	1.23	1.03	1.19	1.15	0.93	0.86	0.90	0.92	0.82	0.91	0.84
MgO	5.86	6.53	3.43	6.68	6.27	6.19	4.98	6.60	4.64	5.06	5.23	6.39	5.44	4.43	5.39	4.94	5.89
CaO	20.73	21.03	18.31	21.60	21.17	20.88	19.67	21.32	19.52	19.95	10.11	10.44	10.25	10.51	10.39	10.38	10.42
Na_2O	1.76	1.52	2.02	1.14	1.45	1.64	1.77	1.33	1.89	1.58	3.20	3.11	2.93	3.16	3.09	3.04	3.10
K_2O	0.01	0.10	0.09	0.03	0.02	0.06	0.09	0.06	0.05	0.06	1.49	1.26	1.44	1.23	1.51	1.34	1.39
Cr_2O_3	0.07	0.00	0.02	0.12	0.10	0.35	0.01	0.06	0.05	0.07	0.02	0.01	0.01	0.01	0.04	0.01	0.02
Total	96.54	96.26	96.28	99.24	97.91	96.71	96.26	97.74	96.42	97.76	96.34	97.54	97.74	99.07	98.01	98.42	97.77
	Cations normalized to 6 oxygens										Cations normalized to 23 oxygens						
Si	1.95	1.98	1.92	1.96	1.98	1.97	1.95	1.96	1.97	1.97	6.28	6.19	6.21	6.17	6.17	6.19	6.18
Ti	—	—	—	—	—	—	—	—	—	—	0.35	0.36	0.35	0.58	0.34	0.47	0.35
Al^{IV}	0.05	0.05	—	0.04	0.01	0.05	0.05	0.04	0.03	0.03	1.77	1.84	1.75	1.66	1.85	1.84	1.85
Al^{VI}	—	—	0.05	—	0.04	—	—	0.01	0.01	0.01	0.11	0.13	0.22	0.21	0.11	0.12	0.12
Fe[a)]	0.57	0.53	0.73	0.56	0.58	0.57	0.64	0.57	0.64	0.64	3.28	2.97	3.15	3.10	3.26	3.12	3.12
Mn	0.03	0.03	0.04	0.03	0.03	0.03	0.03	0.03	0.03	0.03	0.13	0.11	0.12	0.12	0.11	0.12	0.11
Mg	0.36	0.42	0.19	0.41	0.36	0.36	0.30	0.42	0.30	0.30	1.25	1.50	1.28	1.03	1.27	1.16	1.39
Ca	0.89	0.90	0.80	0.92	0.91	0.90	0.87	0.90	0.86	0.86	1.73	1.76	1.74	1.76	1.77	1.75	1.76
Na	0.15	0.16	0.16	0.08	0.08	0.16	0.16	0.08	0.16	0.16	0.99	0.95	0.90	0.96	0.95	0.93	0.95
K	—	—	—	—	—	—	—	—	—	—	0.30	0.25	0.29	0.24	0.31	0.27	0.28
Na_B	—	—	—	—	—	—	—	—	—	—	0.15	0.16	0.16	0.07	0.17	0.16	0.17
$(Na+K)_A$	—	—	—	—	—	—	—	—	—	—	0.98	0.96	0.97	1.05	1.15	0.95	0.94
$Fe^{2+}/(Fe^{2+}+Mg)$	—	—	—	—	—	—	—	—	—	—	0.72	0.66	0.71	0.77	0.72	0.72	0.66
Wo	48.38	47.71	45.73	48.03	48.38	48.38	46.97	46.88	46.97	46.97	—	—	—	—	—	—	—
En	19.23	22.13	10.61	21.27	19.23	19.23	16.34	21.74	16.34	16.34	—	—	—	—	—	—	—
Fs	32.39	30.16	43.66	30.70	32.39	32.39	36.69	31.38	36.69	36.69	—	—	—	—	—	—	—

a) Total Fe.

Table 2 Major (%), trace (μg/g) element and Sr-Nd isotopic compositions of the Maomaogou alkali-feldspar syenites (82-427)[a)]

Sample	Sm-1	Sm-2	Sm-3	Sm-4	Sm-5	Sm-6	Sm-7	Sm-8
SiO_2	54.92	57.08	58.00	58.08	57.28	56.75	56.10	56.59
TiO_2	0.29	0.59	0.38	0.38	0.20	0.54	0.43	0.46
Al_2O_3	22.02	19.94	17.57	22.06	21.31	21.63	21.59	20.35
Fe_2O_3	2.77	4.36	6.00	2.61	4.89	1.61	1.53	2.02
FeO	1.68	1.06	1.52	1.79	1.00	2.94	2.25	3.22
MnO	0.14	0.18	0.33	0.16	0.20	0.10	0.10	0.11
MgO	0.32	0.90	0.16	0.16	0.08	0.44	0.39	0.82
CaO	1.79	3.00	1.08	1.08	0.72	2.27	2.39	2.69
Na_2O	12.01	8.96	7.51	7.97	8.16	9.25	11.45	9.07
K_2O	3.17	2.80	4.64	3.51	4.95	2.91	3.08	3.57
P_2O_5	0.08	0.23	0.10	0.12	0.10	0.14	0.10	0.20
Total	99.20	99.11	98.81	98.26	99.36	98.58	99.41	99.10
P	683.15	969.6	396.7	972.5	817.07	899.44	739.36	900.16
Sc	12.71	2.22	23.2	8.12	6.15	7.79	5.16	9.27
V	11.78	20.36	3.19	19.2	15.23	17.63	13.29	17.34
Ti	2636	3465	1807	3472	3051	3261	2841	3262
Cr	7.46	11.07	3.85	12.08	12.07	10.67	12.06	10.92
Mn	1207.9	1364.3	1051.5	1350.9	1274.1	1318.5	1235.7	1315.2
Co	4.26	5.79	2.73	5.95	5.09	5.49	4.65	5.53
Ni	4.50	6.84	2.16	7.68	6.11	6.67	5.32	6.88
Ga	21.81	23.02	20.6	21.9	21.87	22.16	21.86	21.87
Ge	1.33	1.41	1.25	1.56	1.43	1.46	1.37	1.50
Rb	61.04	61.13	60.94	61.52	59.79	61.30	58.93	61.39
Sr	425.75	604.2	247.3	638.2	530.13	576.59	476.09	585.09
Y	18.42	24.55	12.3	24.78	21.59	23.13	20	23.19
Zr	133.33	168.1	98.56	172.2	152.96	161.46	143.34	162.48
Nb	31.03	43.86	18.19	44.31	38.95	40.88	36.28	40.99
Ba	1701.6	1605.5	1797.6	1679.4	1699.7	1666.5	1709.9	1684.9
La	22.45	30.35	14.55	30.04	25.72	28.22	23.56	28.14
Ce	41.2	58.4	24	58.66	49.92	54.23	45.55	54.29
Pr	4.86	6.92	3.09	7.04	5.96	6.39	5.42	6.49
Nd	16.85	23.12	10.58	23.8	20.13	21.89	18.29	22.06
Sm	3.07	4.25	1.89	4.45	3.75	4.05	3.40	4.10
Eu	1.10	1.48	0.72	1.62	1.35	1.46	1.22	1.49
Gd	2.99	4.18	1.82	4.09	3.49	3.84	3.19	3.82
Tb	0.53	0.73	0.32	0.71	0.61	0.67	0.56	0.67
Dy	3.07	4.19	1.95	4.46	3.81	4.04	3.48	4.11
Ho	0.63	0.84	0.43	0.89	0.77	0.81	0.71	0.83
Er	1.88	2.48	1.28	2.46	2.16	2.32	2.01	2.31
Tm	0.29	0.37	0.21	0.38	0.34	0.35	0.31	0.36
Yb	1.98	2.47	1.49	2.64	2.33	2.43	2.18	2.47
Lu	0.32	0.39	0.26	0.43	0.38	0.39	0.36	0.40
Hf	3.51	4.51	2.51	4.40	3.93	4.20	3.69	4.17
Ta	2.31	2.97	1.65	3	2.97	2.82	2.96	2.83
Pb	6.98	7.39	6.56	7.42	7.01	7.30	6.80	7.31
Th	3.46	4.81	2.12	4.02	3.55	4.07	3.31	3.88
U	0.72	0.69	0.74	0.72	0.69	0.71	0.67	0.72
LREE/HREE	2.97	3.09	2.73	3.07	3.01	3.06	2.97	3.05
ΣREE	101.22	139.85	62.59	141.68	120.73	131.11	110.25	131.57
dEu	1.09	1.06	1.17	1.14	1.12	1.11	1.13	1.11
$^{143}Nd/^{144}Nd$			0.512537±13					
$e_{Nd}(T)$			0.57					
$^{87}Sr/^{86}Sr$			0.706011±7					
$e_{Sr}(T)$			−7.1					

a) Major elements were determined by wet analyses at the Institute of Geochemistry, Chinese Academy of Sciences, Guiyang. Trace elements (include REE) and Nd-Sr isotopic compositions were measured respectively by ICP-MS and MC-ICP-MS at the Institute of Geochemistry, Chinese Academy of Sciences, Guangzhou. The measurement accuracy and method are described in refs. [8, 9].

Al_2O_3, alkali-rich (($Na_2O + K_2O$ averaging 13.13%)), high Na_2O ($Na_2O > K_2O$). As shown in Fig. 2, on the total alkalis versus silica (TAS) plot[6], all samples fall in the alkaline field; while on the K_2O versus SiO_2 plot[7], all samples fall in the sodium alkaline field, consistent with that on TAS plot. Therefore, Maomaogou alkali-feldspar syenites could be concluded to be sodium alkaline rocks. In the primitive mantle-normalized spidergrams (Fig. 3(a)), all samples are enriched Pb and large-ion lithophile elements (LILE) such as K, Rb, Ba, and depleted high-field-strength elements (HFSE) such as Nb, Ta, Ti. The REE contents are in the range of 62.59—141.68 μg/g, showing enrichment light REE (LREE/HREE = 7.06—7.95) (Fig. 3(b)). Eu displays mild anomaly and the δEu values are between 1.06 and 1.17. Sr and Nd isotopic compositions display that the Maomaogou lavas originated from the tiny depleted-mantle source ($\varepsilon_{Nd}(T)$ = + 0.57 and $\varepsilon_{Sr}(T)$ = –7.1).

2 Analytical methods

(i) Zircon grains sorting. In order to eliminate the contamination as fully as possible, the following method is applied to separating zircon grains.

About 0.5 kg sample (82-427) is broken up into small pieces with each being 1 cm^3, then put it in the stainless steel bowl whose diameter is about 20 cm, and grind it for 3—5 s in XZW 100 vibration grinder (1.1/0.75 Kw). Repeat the grinding until all of the samples pass through the pore diameter sieve of about 0.3 mm. Wash the dust out, enrich the heavy mineral with aluminous pan. By making magnetic and electromagnetic selection, non-magnetic heavy mineral is left, the zircon concentrates are gained by another elutriation at last, representative zircon grains were handpicked under a binocular microscope.

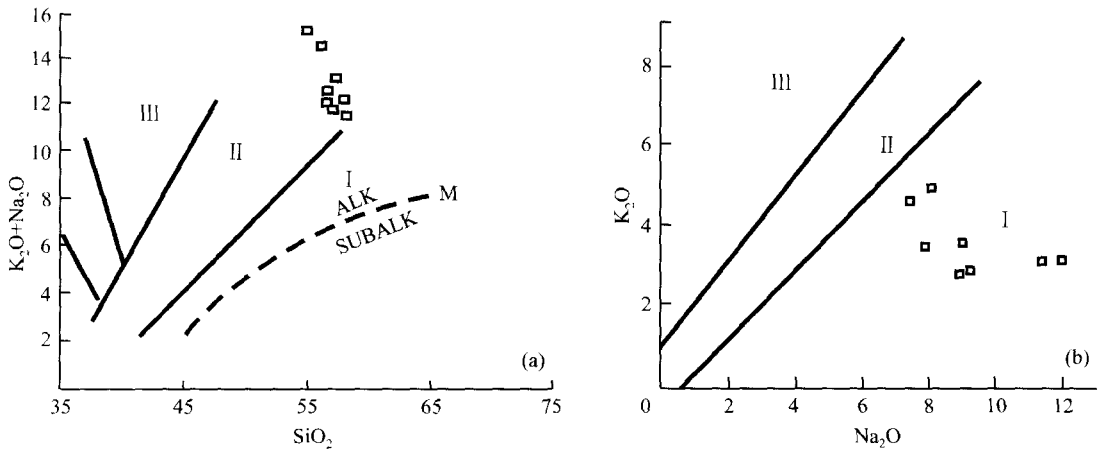

Fig. 2. Total alkalis vs. SiO_2 (a) and K_2O vs. Na_2O (b) diagrams of the Maomaogou alkaline rocks. (a) I, Weak alkaline rock section; II, middle alkaline rock section; III, fens alkaline rock section. (b) I, Sodium alkalic rock section; II, transition alkalic rock section; III, potassium alkalic section.

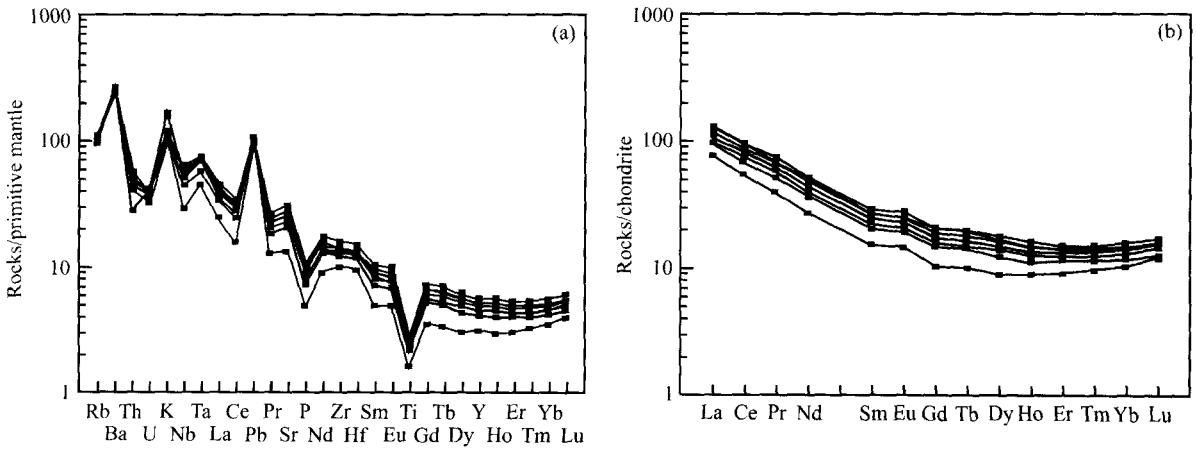

Fig. 3. Primitive mantle-normalized trace elemental diagrams (a) and chondrite-normalized rare earth elements patterns (b) of the Maomaogou alkali-feldspar syenites. The mantle-normalization values are from ref. [10].

(ii) Analytical methods. The U-Pb analyses were performed using the Sensitive High-Resolution Ion Microprobe (SHRIMP II) at the Chinese Academy of Geological Sciences in Beijing. Execution of sample target, operation and data processing procedures have been described by refs. [11—13]. Internal structure was examined using cathodoluminescence (CL) images prior to U-Pb isotopic analyses (Fig. 4). The interelement fractionation in ion emission of zircon was corrected by using RSES referenced zircon TEM (417 Ma), and U, Th and Pb concentrations were determined based on the standard Sri Lankan gem zircon SL3, which has a U concentration of 238 μg/g corresponding to an age of 572 Ma. Common Pb was corrected by using observed ^{204}Pb. Uncertainties of data points listed in Table 3 are given at ±1*s*. The ages quoted in the text are ^{206}Pb/^{238}U (the older age is ^{207}Pb/^{206}Pb ages) ages, which are the weighted mean at the 95% confidence level. The software of Ludwig SQUID 1.0 and attached ISOPLOT were used for data processing.

(iii) Results. Analyzed zircons are mostly colorless, transparent, euhedral, stubby, tetragonal dipyramid with length∶width ratios from 2∶1 to 3∶1. CL images clearly show that most of the zircons are magmatic compound zircons[1)] which have relict inner cores and growing outer shells. The results of zircon SHRIMP U-Pb analyses for Maomaogou alkali-feldspar syenite are listed in Table 3 and illustrated on the concordia plot in Fig. 5. As shown in Table 3, Th, U concentrations of 15 labels, range from 28 to 353 μg/g and 139 to 1607 μg/g, respectively. Th/U ratios of these analyses vary in the range of 0.07—0.73. Both core and shell of every magmatic compound zircon undergo the SHRIMP U-Pb dating. Of the 15 analyses, 7 fall within a single group spreading slightly along the concordia, yielding a weighted mean ^{206}Pb/^{238}U age of 224±8 Ma (MSWD = 2.6) (Table 3, Fig. 5(b)). The age records the crystallization time of the Maomaogou alkali-feldspar syenite. At the same time, two old age periods of relict cores of zircon are determined, they are the Archean age (2692—2818 Ma) and Neoproterozoic age (622—691 Ma), which are interpreted as the ages of exotic zircons from the Neoproterozoic and Archean basement respectively. From the positions of measured plots (Fig. 4(c) and (f)), 841 ± 18 and 438 ± 9 Ma are likely to be the ages of transition section between cores and shells, so the two ages have not geological implication.

3 Discussion

(i) Formation ages of the Maomaogou alkali-feldspar syenites. Except that a few zircons (Fig. 5(a)) are the crystalline magmatic zircons after emplacement, most of the dating zircons are magmatic compound zircons in the Maomaogou alkali-feldspar syenite. The measured spots of the magmatic zircon and magmatic compound zircons are selected in the center part and the shell having the rhythmic zone respectively. Seven analyses have concordant ^{206}Pb/^{238}U ages, which correspond to a single age population with a weighted mean ^{206}Pb/^{238}U age of 224 ± 8 Ma (MSWD = 2.6). The age records the crystallization time of the Maomaogou alkali-feldspar syenite. Thus, the Maomaogou alkali-feldspar syenites were formed in the late Triassic corresponding to Indosinian epoch. Comparing the new data with the biotite K-Ar age of 260 Ma[4]

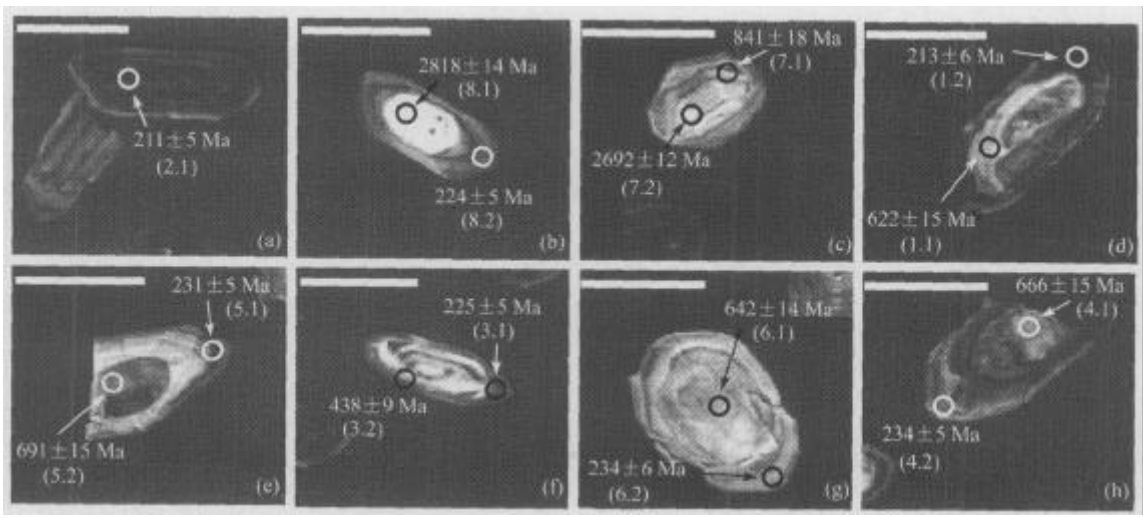

Fig. 4. CL images of zircons from the Maomaogou alkali-feldspar syenites. Circle and number denote the spot center and age. Magmatic zircon (a) and magmatic compound zircons ((b)—(h)), and the length of scale bar is 100 μm. 7.2 and 8.1 are the ^{207}Pb/^{206}Pb ages and the others are ^{206}Pb/^{238}U ages.

1) Zhang, Y. Q., Xia, B., Liang, H. Y. et al., The characters of dating zircons and its geological implications, Geological Journal of China Universities, 2004 (in press).

Table 3 SHRIMP U-Pb isotopic data for zircons from the Maomaogou alkali-feldspar syenites (82-427)[a)]

Spot	Type	Pb_c (%)	U /10^{-6}	Th /10^{-6}	Th /U	$^{206}Pb^*$ /10^{-6}	$^{207}Pb/^{206}Pb$ (±%)	$^{207}Pb/^{235}U$ (±%)	$^{206}Pb/^{238}U$ (±%)	Ages/Ma	
										$^{206}Pb/^{238}U$	$^{207}Pb/^{206}Pb$
1.1	c	0.00	639	52	0.08	56	0.077 ± 1.3	1.08 ± 2.9	0.101 ± 2.6	622 ± 15	1122 ± 26
1.2	r	0.00	562	134	0.25	16	0.053 ± 4.4	0.24 ± 5.1	0.034 ± 2.7	213 ± 6	315 ± 99
2.1	r	0.15	16077	256	0.16	46	0.049 ± 1.3	0.23 ± 2.6	0.033 ± 2.3	211 ± 5	213 ± 31
3.1	r	0.94	555	236	0.44	17	0.048 ± 6.4	0.24 ± 6.9	0.036 ± 2.4	225 ± 5	120 ± 150
3.2	t	0.54	382	182	0.49	23	0.055 ± 3.4	0.53 ± 4.1	0.070 ± 2.3	438 ± 9	391 ± 76
4.1	c	0.85	496	353	0.73	46	0.130 ± 1.3	1.95 ± 2.6	0.109 ± 2.3	666 ± 15	2103 ± 22
4.2	r	0.48	1228	175	0.15	39	0.049 ± 3.0	0.25 ± 3.8	0.037 ± 2.4	234 ± 5	137 ± 71
5.1	r	1.61	352	115	0.34	11	0.056 ± 7.1	0.28 ± 7.5	0.036 ± 2.5	231 ± 5	461 ± 160
5.2	c	3.33	916	174	0.20	92	0.127 ± 2.5	1.98 ± 3.4	0.113 ± 2.3	691 ± 15	2054 ± 44
6.1	c	0.37	411	37	0.09	37	0.076 ± 2.7	1.10 ± 3.6	0.105 ± 2.4	642 ± 14	1106 ± 55
6.2	r	1.93	396	28	0.07	13	0.050 ± 7.5	0.25 ± 7.9	0.037 ± 2.5	234 ± 6	199 ± 170
7.1	t	0.25	745	267	0.37	89	0.079 ± 2.4	1.52 ± 3.3	0.139 ± 2.3	841 ± 18	1171 ± 47
7.2	c	0.13	495	172	0.36	161	0.184 ± 0.7	9.58 ± 2.4	0.377 ± 2.3	2063 ± 41	2692 ± 12
8.1	c	0.28	139	79	0.58	54	0.199 ± 0.9	12.29 ± 2.6	0.448 ± 2.4	2386 ± 48	2818 ± 14
8.2	r	1.21	670	139	0.21	21	0.056 ± 4.5	0.27 ± 5.1	0.035 ± 2.3	224 ± 5	436 ± 100

a) c, Core; r, shell; t, the transition between cores and shells. Pb_c and Pb* indicate the common and radiogenic portions, respectively; error in the standard calibration was 1.07%; common Pb is corrected using measured ^{204}Pb.

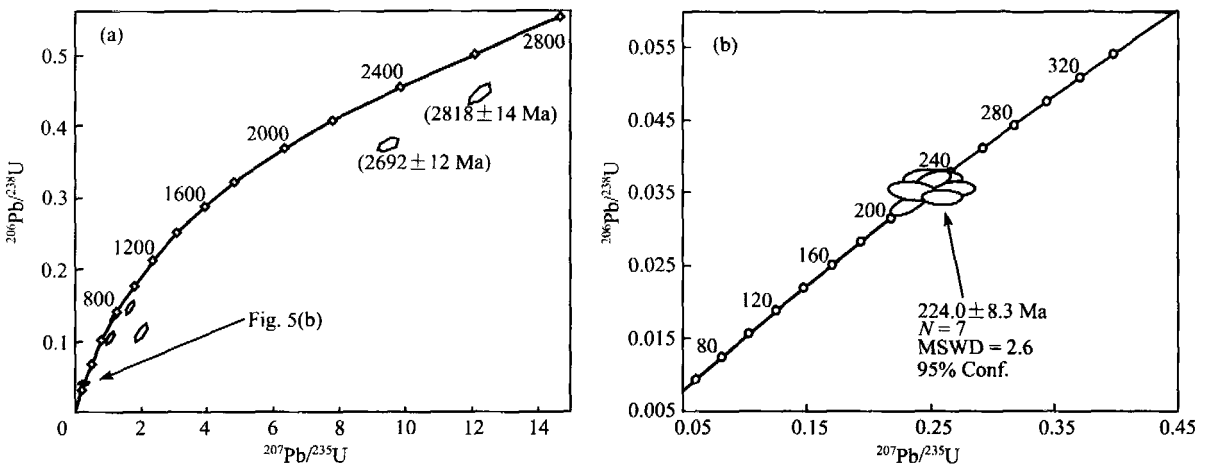

Fig. 5. SHRIMP zircon U-Pb concordia diagrams for the Maomaogou alkaline feldspar syenites. (a) Plot of all data, (b) enlarged lower part of Fig. 5(a).

and $^{40}Ar/^{39}Ar$ plateau age of 252 Ma[5], the reported ages are far older than the zircon SHRIMP U-Pb age.

(**ii**) The origin of Maomaogou alkali-feldspar syenite. The geochemical characteristics such as LILE enrichment and HFSE depletion and the Nd-Sr isotopic compositions ($e_{Nd}(T)$ = +0.57 and $e_{Sr}(T)$ = −7.1) preclude that the Maomaogou alkali-feldspar syenites are the partial melting products originating from the sodium alkali-rich tiny depleted-mantle source.

(**iii**) Collating and stipulating the time of rock-control tectonic tension. In Panxi area, the magmatic rocks with the rifting include alkaline plutonic rocks (e.g. alkali-feldspar syenite in Maomaogou from Huili County), igneous rocks and mafic-ultramafic layered intrusions. The alkaline plutonic rocks trend N-S, being more than 300 km long[2,14]. In recent years, there have been several attempts to date the magmatic rocks in Panxi: Lo et al.[5] obtained whole-rock ^{40}Ar-^{39}Ar plateau age of 252 Ma for Emeishan basalt[5]. Zhou et al.[15] reported the zircon SHRIMP U-Pb age of 259 Ma for layered intrusions, and Liu et al.[16] recorded 215 Ma using the zircon ELA-ICP-MS dating method for layered intrusions. All the isotopic geological ages vary in the range of 259—215 Ma, which reveal that the time of intense tension of Panxi rift is from the late Permian to the late Triassic. This report presents zircon SHRIMP U-Pb dating results of 224±8 Ma on the alkaline plutonic rocks from Maomaogou, which also support the preceding conclusion.

(iv) Discovery of the late Archean residual zircons. Most of the dating zircons are magmatic compound zircons in the Maomaogou alkali-feldspar syenites generating in extensional tectonics. The results indicate that the crystallization time of Maomaogou alkali-feldspar syenites is 224 ± 8 Ma. At the same time, the late Archean age of 2818 Ma was determined, which is the oldest age of residual zircons in the middle part of Kangdian old-land, western Yangtze Block, while the SHRIMP U-Pb zircon age of Suxiong volcanics was 803 ± 12 Ma in this area[17]. The discovery thus provides the precise evidence for the presence of Archean basement in the Kangdian old-land. In addition, the residual zircons ages of 3.2—3.3 Ga[18−20] have been obtained on the granites and the volcanic rocks all around the Yangtze Block recently, which show that the Neoproterozoic magmatic rocks are distributed around the Yangtze Block and also there would be a residual Archean basement in the region.

(v) The possible reason that the biotite 40Ar/39Ar plateau age is older than the zircon SHRIMP U-Pb age. The biotite $^{40}Ar/^{39}Ar$ plateau age of 252 Ma is far older than the zircon SHRIMP U-Pb age in Maomaogou alkali-feldspar syenites, which is not caused by dating methods but likely caused by the existing of excess Ar in alkaline plutonic rocks. Alkali-plutonic rocks were formed under high temperature and high pressure conditions, and the plutonic rocks are ongoing under deeper closed system. Consequently, the gases including argon (Ar) could not volatilize in preceding stages, and were preserved into the mineral crystal lattices, e.g. pyroxene, biotite, which have crystallized early. And this is the origin of excess argon and very likely the reason that leads the age to become older.

Acknowledgements The authors are greatly indebted to the anonymous reviewers, and Profs. Wang Dezi, Liu Dunyi, Wu Jiashan, Zhou Jianxiong, Zhong Dalai and Xu Ronghua for their helpful comments on the manuscript. They would like to thank Prof. Shi Yuruo for enthusiastic help in SHRIMP II zircon U-Pb analyzing and Prof. Li Shunrong for major elements analyzing. This work was supported by the Knowledge Innovation Program of the Chinese Academy of Sciences (Grant Nos. KZCX2-SW-117 and KZCX2-101).

References

1. Petro, W. L., Vogel, T. A., Wilband, J. T., Major-element chemistry of plutonic rock suites from compressional and extensional plate boundaries, Chemical Geology, 1979, 26: 217—235.
2. Shi, Z. M., Li, W. G., Zhang, Y. C., Ring Alkalic Complexes of the Panxi Rift Zone, Contribution to Panzhihua-Xichang Rift China No.1 (ed. Zhang, Y. X.) (in Chinese), Beijing: Geological Publishing House, 1985, 175—200.
3. Liu, B. G., Li, Y. G., Ding, K. S., Alkaline Rocks, the Forming and Evolvement of Panxi Rift (ed. Cong, B. L.) (in Chinese), Beijing: Science Press, 1988, 287—309.
4. Zhang, Y. Q., Xie, Y. W., The Geochemistry of Granite from Hengduanshan Area (in Chinese), Beijing: Science Press, 1995, 30—33.
5. Lo, C. H., Chung, S. L., Lee, T. Y. et al., Age of the Emeishan flood magmatism and relations to Permian-Triassic boundary events, Earth and Planetary Science Letters, 2002, 198: 449—458.
6. Miyashiro, A., Nature of alkalic rock series, Contrib. Mineral. Petrol., 1978, 66: 91—104.
7. Poucle, A., Contribution a 1a systematique des laves alkaline, les laves du rift de I'Afrique Centrale (Zaire-Uganda), Bull. Volcanol, 1980, 43: 527—551.
8. Liu, Y., Liu, H. C., Li, X. H., Simultaneous and precise determination of 40 trace elements in rock samples using ICP-MS, Geochimica (in Chinese), 1996, 25(6): 552—558.
9. Liang, X. R., Wei, G. J., Li, X. H. et al., Pricise measurement of $^{143}Nd/^{144}Nd$ and Sm/Nd ratios using multiple-collectors inductively coupled plasma-mass spectrometer (MC-ICPMS), Geochimica (in Chinese), 2003, 32 (1): 91—96.
10. Sun, S. S., McDonough, W. F., Chemical and isotopic systematics of oceanic basalts: Implications for mantle composition and processes, Magmatism in the Ocean Basins (ed. Saunders, A. D., Norry, M. J.), Geol. Soc. Special Publications, 1989, 42: 313—314
11. Composton, W., Williams, I. S., Meyer, C., U-Pb geochronology of zircons from lunar breccia 73217 using a sensitive high mass-resolution ion microprobe, J. Geophys. Res., 1984, 89: B525—B534.
12. Williams, I. S., Some observations on the use of zircon U-Pb geochronology in the study of granitic rocks, Trans. R. Soc. Edinburgh-Earth Sci., 1992, 83: 447—458.
13. Song, B, Zhang, Y. H., Wan, Y. S. et al., Mount making and procedure of the SHRIMP dating, Geological Review (in Chinese), 2002, 48 (supp): 26—30.
14. Zhou, B. F., Shi, Z. M., Zhang, Y. C. et al., A-type Granites of the Panxi Zone, Contribution to Panzhihua-Xichang Rift China, No.1 (eds. Zhang, Y. X.) (in Chinese), Beijing: Geological Publishing House, 1985, 201—221.
15. Zhou, M. F., John, M., Song, X. Y. et al, A temporal link between the Emeishan large igneous province (SW China) and the end-Guadalupian mass extinction, Earth and Planetary Science Letters, 2002, 196: 113—122.
16. Liu, H. Y., Xia, B., Liang, H. Y. et al., Geochronology of layered intrusions in Cida and Taihe districts, Panxi area, Sichuan Province, Geological Journal of China Universities (in Chinese), 2004, 10(2): 179—185.
17. Li, X. H., Zhou, H. W., Li, Z. X. et al., Zircon U-Pb age and Petrochemical characteristics of the neoproterozoic bimodal volcanics from western Yangtze block, Geochimica (in Chinese), 2001, 30(4): 315—322.
18. Qiu, Y. M., Gao, S., McNaughton, N. J. et al., First evidence of > 3.2 Ga continental crust in the Yangtze craton of south China and its implications for Archean crustal evolution and Phanerozoic tectonics, Geology, 2000, 28 (1): 11—14.
19. Zhang, Q., Jian, P., Liu, D. Y. et al., SHRIMP dating of volcanic rocks from Ningwu area and its geological implications, Science in China, Series D, 2003, 46(8): 830—837.
20. Zheng, Y. F., Neoproterozoic magmatic activity and global change, Chinese Science Bulletin, 2003, 48 (16): 1639—1656.

(Received March 1, 2004; accepted April 29, 2004)